Photoconductivity and Charge-Carrier Photogeneration in Photorefractive Polymers

Däubler, Thomas K.; Kulikovsky, Lazar; Neher, Dieter; Cimrová, Vera; Hummelen, Jan; Mecher, Erwin; Bittner, Reinhard; Meerholz, Klaus

Published in:
Nonlinear optical transmission processes and organic photorefractive materials

Publication date:
2002

Photoconductivity and Charge-Carrier Photogeneration in Photorefractive Polymers

Thomas K. Däubler [a], Lazar Kulikovsky [b], Dieter Neher [b*], Vera Cimrová [c], J.C. Hummelen[d]
Erwin Mecher [e], Reinhard Bittner [e], Klaus Meerholz [e]

[a] Schott Spezialglas GmbH, Div. Luminescence Technology, Hattenbergstr. 10, 55014 Mainz, Germany

[b] Institut für Physik, Universität Potsdam, Am Neuen Palais 10, D-14469 Potsdam, Germany

[c] Institute of Macromolecular Chemistry, Academy of Sciences of the Czech Republic, 16206 Prague 6, Czech Republic

[d] Stratingh Institute and Materials Science Center, University of Groningen Nijenborgh 4, 9747 AG Groningen, The Netherlands

[e] Institut für Physikalische Chemie, Universität München, Butenandtstr. 5-13, D-81377 München, Germany

[*] neher@rz.uni-potsdam.de

ABSTRACT

We have studied photogeneration, transport, trapping and recombination as the governing mechanisms for the saturation field strength and the time response of the photorefractive (PR) effect in PVK-based PR materials, utilizing xerographic discharge and photoconductivity experiments. Both the charge carrier photogeneration efficiency and the photocurrent efficiency were found to be independent of chromophore content, suggesting that the chromophore does not participate in carrier generation and trapping. The photoconductivity gain factor G defined as the number of charge carriers measured in photoconductivity in relation to the number of carriers initially photogenerated as determined by the xerographic experiments is found to be much smaller than unity, which indicates that the mean free path of the photogenerated charge carriers is less than the grating period. Photoconductivity data can be explained over 3 orders of magnitude in field, assuming a field-independent trap density. Based on the photoelectric data, PR response times have been predicted by Yeh's model for the build-up of space or by calculating the time, which is necessary to fill all traps by photogenerated holes. Only the latter model can reasonably well explain the observed field dependence of the PR growth time, suggesting that trap -filling essentially controls the PR onset behaviour.

Keywords: photorefractivity, Schildkraut model, space-charge field, trap density, response time, xerography

1. INTRODUCTION

The photorefractive (PR) effect is defined as the spatial modulation of the index of refraction in an electro-optically active material due to the redistribution of charge carriers photogenerated under non-uniform illumination. For the build-up of the refractive index grating the following processes are necessary: (i) photogeneration of charge carriers, (ii) diffusion or drift of the mobile charge carriers, (iii) trapping of these charge carriers in the regions of low light intensity

Nonlinear Optical Transmission Processes and Organic Photorefractive Materials,
Christopher M. Lawson, Klaus Meerholz, Editors, Proceedings of SPIE
Vol. 4462 (2002) © 2002 SPIE · 0277-786X/02/$15.00

and (iv) change of the index of refraction due to the build-up of an internal space-charge field. To relate a material's PR performance to these fundamental processes, (i) and (ii) can be studied by photoconductivity [1-3]. The electro-optical response has been investigated with ellipsometric techniques [4].

In contrast to these intensively studied processes, charge trapping in PR polymers is less well understood. Even though trap densities have been extracted from two-beam coupling (2BC) experiments [5-7], few attempts have been made to identify the trapping sites and to apply independent techniques to determine their density. Recently, absorption spectroscopy was used to determine the C_{60} radical anion concentration in C_{60}-sensitized PR polymers based on the photoconductor poly(*N*-vinylcarbazole) (PVK) [8]. It was concluded that C_{60}^- acts as the primary hole trap. Trap densities determined by this simple spectroscopic method were in good agreement with those inferred from 2BC experiments. In analogy to the model for PVK/C_{60}, West *et al.* proposed a trapping mechanism for a PVK/TNF system [9]. However, in this work no independent technique was employed to determine the trap density and the proposed model is merely based on the comparison of blends containing different chromophores. In a polysiloxane/TNF system photoconductivity experiments were used to independently determine the density of recombination centers [10]. The charged recombination sites were identified with occupied deep traps and their density was in reasonable agreement with calculations from 2BC experiments. It should be noted that in most cases, trap densities (as determined from 2BC in combination with DFWM) were estimated using the standard model for the photorefractive effect that was originally developed for inorganic PR crystals [11,12].

In this paper we investigate the photoresponse of PVK-based PR materials by photoconductivity (PC) and xerographic discharge (XD) experiments. By completing the characterization of the fundamental processes involved in the PR effect, a consistent picture of the photoconductivity, the charge carrier photogeneration efficiency, and the PR performance of PVK-based PR materials is provided. While the XD technique is known to be the most accurate method to determine the charge carrier photogeneration efficiency [13,14], the transport and trapping properties of the materials can be addressed by PC experiments. Using Schildkraut's model for the space-charge-field formation in organic PR materials [15] a relation between the trap density and the photoconductivity gain is elaborated. This analysis is used to estimate the space-charge field in the studied PR materials. Furthermore, the results are combined with Yeh's model for the fundamental limit of speed for the PR grating formation [16] and compared with response times derived from DFWM experiments on PVK-based PR materials. Finally, the time which is required to fill all traps with photogenerated carriers is shown to limit for the growth rate of the PR signal.

2. EXPERIMENT

The investigated PR materials are based on the photoconductor poly(*N*-vinylcarbazole) (PVK), the electro-optic chromophore 2,5-dimethyl-4-(*p*-nitrophenylazo)anisole (DMNPAA) and the plasticizer *N*-ethylcarbazole (ECZ). 2,4,7-trinitro-9-fluorenone (TNF) and a soluble C60 derivative, [6,6]-phenyl-C61-butyricacid-methylester (PCBM), were used as photosensitizers (Fig. 1).

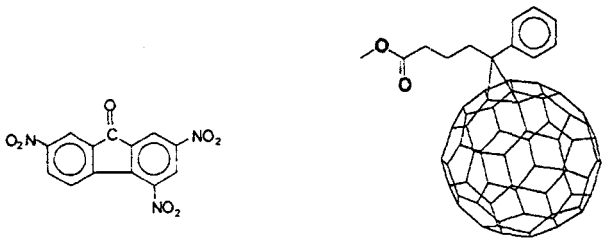

Fig. 1. Chemical structure of the two photosensitizers TNF and PCBM used in this study.

PVK secondary standard, TNF and ECZ were purchased from Aldrich Chemie GmbH. ECZ was purified by recrystallization while PVK was used without further purification. DMNPAA was synthesized by azo-coupling of a

para-nitroaniline-diazonium salt with dimethylanisole and purified by column chromatography. PCBM was synthesized according to Ref 17. T_gs of the blends were varied by changing the ratio of PVK/ECZ.

The devices for photoconductivity (PC) experiments were prepared identical to those used for DFWM and 2BC experiments by melt-pressing. The blends were sandwiched between two ITO-coated glass substrates at elevated temperature using 37 μm glass spacer beads to adjust the film thickness *L*. A strict preparation and measurement protocol was obeyed to obtain reproducible results [18]. Samples for xerographic discharge experiments were prepared by spincoating from chloroform solution on polished stainless steel substrates. The thickness of the polymer layer was typically 1 - 2 μm.

Current-voltage (I-V) characteristics were recorded in dry nitrogen atmosphere in a temperature stabilized setup [19]. For experiments under illumination a 689 nm diode laser with a photon flux of about 5×10^{17} photons/cm^{2}s was used. Data were recorded pointwise and refer to currents established after the respective bias voltage was applied for 30 s. Dark currents, measured as a function of the electric field before and after experiments under illumination, were subtracted from currents measured under illumination to give the field dependence of the photocurrent ($j_{photo} = j_{light} - j_{dark}$). In the study presented here, the current was measured with a Keithley 237 source measure unit for voltages between -1000 V to 1000 V. For larger bias, a Heinziger high-voltage source was used in combination with the Keithley 617 electrometer. All photocurrent data were recorded at a temperature equivalent to the glass transition temperature of the material.

Xerographic discharge (XD) experiments were performed with a home-build setup [14]. The sample was charged to the initial surface potential $U(t_0)= Q(t_0)/C$ by corona and then discharged upon irradiation. Here, $Q(t_0)$ is the surface charge density and C is the sample capacitance per unit area. $U(t)$ was recorded with a sampling frequency of 50 Hz. The photoinduced discharge quantum efficiency η' is calculated from

$$\eta' = -\frac{1}{eF}\left(\frac{dQ}{dt}\right)_{t0} = -\frac{1}{eF}C\left(\frac{dU}{dt}\right)_{t0} \qquad (1)$$

where Φ is the absorbed photon flux density, e is the electron charge, $(dQ/dt)_{t0}$ represents the rate of change of the surface charge density and $(dU/dt)_{t0}$ is the initial photoinduced discharge rate. Under emission-limited conditions, η' is independent of both sample thickness and light intensity and equals the charge carrier photogeneration efficiency η. To ensure emission-limited conditions, the incident photon flux was kept as low as possible (10^{13} - 10^{14} photons/cm^{2}s). A halogen lamp with various interference filters was used for illumination, except at 355 nm, for which a UV-MAG lamp was used. The measurements were performed with illumination upon the positively charged surface. All experiments were carried out under ambient conditions.

Degenerate four-wave mixing experiments were performed in the typical tilted geometry with a wavelength of 633 nm. Two s-polarized write beams ('1' and '2') with external angles α_1 = 50° and α_2 = 70° relative to the sample normal were overlapped in 105 μm thick polymer films sandwiched between ITO-coated glass electrodes. Readout was performed by a weak p-polarized probe beam counter-propagating to beam '1'. The transmitted $I_{R,trans}$ and diffracted $I_{R,diffr}$ components of the read beam were monitored by photodiodes. The external diffraction efficiency is defined as $\eta_{ext} = I_{R,diffr}/I_{R,ext}$; the internal diffraction efficiency was calculated according to $\eta_{\mathrm{int}} = I_{R,diffr}/(I_{R,diffr} + I_{R,trans})$ and is related to the refractive index modulation amplitude according to $\Delta n = \lambda \cos\alpha_{1,\mathrm{int}}\, \alpha \sin(\sqrt{\eta_{\mathrm{int}}})/(\pi d)$. Here, d is the sample thickness, and λ the laser wavelength.

3. PHOTOCONDUCTIVITY

The intensity dependence of the photocurrents ($j_{photo} = j_{light} - j_{dark}$) is compared for different samples in Figure 2a. Blends with different photosensitzer, namely TNF and PCBM are compared. It is observed that j_{photo} of the sample with PCBM is significantly lower than j_{photo} of materials containing TNF.

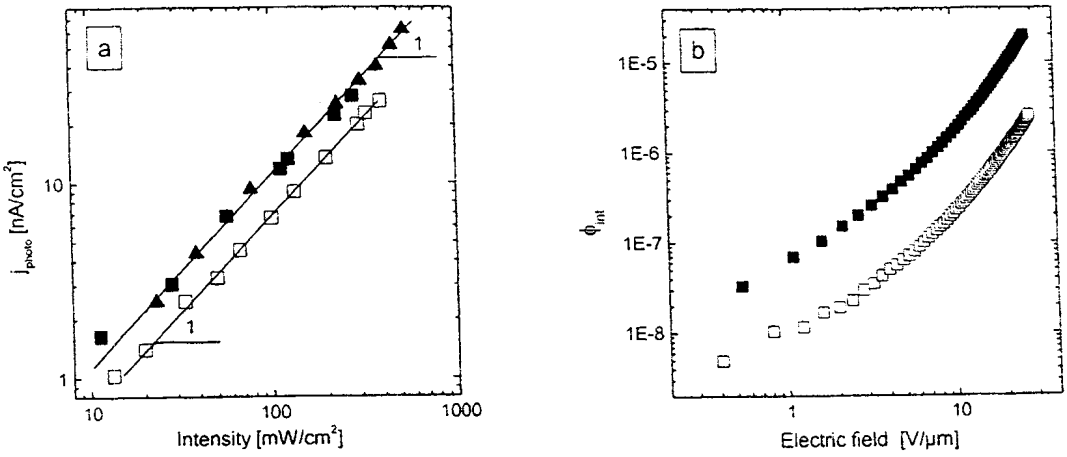

Fig. 2. a) Intensity-dependence of the photocurrents and b) Field-dependence of the internal photocurrent efficiency of 37 µm thick samples of PVK/TNF (50 wt.-% Chrom.) (solid triangles), PVK/TNF (30 wt.-% Chrom.) (solid squares), and PVK/PCBM (30 wt.-% Chrom.) (open squares). Illumination was at 633 nm. In a) the applied electric field was 13 V/µm.

The internal photocurrent efficiency f_{int} of samples with 30 wt.-% chromophore contents and TNF or PCBM as photosensitizer is shown in Figure 2b as a function of electric field. f_{int} is defined as the number of measured charge carriers per absorbed photon:

$$f_{\mathrm{int}} = \frac{hc}{e\,l\,\ln 10\,a_{10}L}\,\frac{j_{photo}}{I} \quad , \tag{2}$$

where I is the light intensity, L the thickness of the sample, α_{10} the absorption coefficient taken to the log base 10, and λ the wavelength of light.

The field-dependence of f_{int} is linear at low fields and quadratic at high fields. f_{int} of blends with PCBM is almost an order of magnitude lower over the entire investigated range in the electric field when compared to blends with TNF, suggesting a more efficient photogeneration in the PVK/TNF charge transfer (CT) complex and less efficient sensitization of PVK by the C_{60} derivative.

In an earlier study we observed a pronounced increase in j_{photo} for samples with $T_g < T_M$ (T_M is the measurement temperature). When plotted as a function of the reduced temperature $T_r = T_g - T_M$, the data showed a universal behavior. Thus, j_{photo} is mainly a function of the temperature with respect to T_g and does not strongly depend on the chromophore or the plasticizer content. This is also illustrated by the intensity dependence of j_{photo} for blends containing 30 wt.-% and 50 wt.-% DMNPAA shown in Fig. 2a, where the absolute values of j_{photo} are identical. Note, that in this work all photocurrents were measured at $T_M = 0$. Thus, the universal T_r-dependence of j_{photo} can only be caused by changes in the charge carrier photogeneration efficiency or in the transport and recombination properties of the materials. Intensity-dependent photoconductivity experiments allow to study the latter processes without changing the photogeneration efficiency. In Fig. 2a the slope for the increase of j_{photo} with intensity is found to be unity for all samples. This clearly indicates that no bimolecular recombination of charge carriers occurs in the materials studied here. This observation favors the interpretation that the universal behavior of j_{photo} with respect to T_r is mainly caused by T_g-dependent changes in the transport properties.

4. CHARGE CARRIER PHOTOGENERATION

Since it is not possible to safely exclude T_g-dependent effects on the charge carrier photogeneration efficiency only by photoconductivity experiments, xerographic discharge measurements have been carried out in addition. The field dependence of the measured charge carrier photogeneration efficiencies η for PR blends with different T_g's and chromophore content is compiled in Figure 3. In the analysis of the xerographic data only the absorption of PVK/TNF was taken into account. Note, that the absorption of the chromophore is still low at 580 nm and does not significantly attenuate the incident light in the approx. 2 µm thick samples. One might presume that the requirement of emission-limited discharge may no longer be fulfilled when irradiating at a wavelength with low absorption i. e., when light penetrates through the whole sample and is not only absorbed in a surface near region. In an earlier study we investigated the effect of penetration depth on the determination of the charge carrier photogeneration efficiency [20]. Our results were in good agreement with data published by Andre *et al.* [21] and showed that h is almost wavelength independent for illumination between 400 nm and 650 nm. This provides evidence that the absolute values of the photogeneration efficiency in the PR blends are correctly determined for the wavelengths of illumination used here.

In Figure 3 no dependence of the h on the chromophore content and the glass-transition temperature can be observed. Since the fraction of photons absorbed by the chromophore varies significantly for the studied samples, the close similarity of the photogeneration efficiencies indicates that the chromophore does not act as a hole acceptor in the direct photogeneration step. XD experiments on blends containing no TNF indeed show much smaller generation efficiencies. The absence of a r_{CHR}-dependence of h confirms the conclusions drawn from photoconductivity experiments. The finding that h is, furthermore, independent of T_g allows to exclude contributions of a T_g-dependent photogeneration efficiency to the universal T_r-dependence of j_{photo}. Thus, the changes in j_{photo} are most likely related to changes in the transport and recombination properties with T_g.

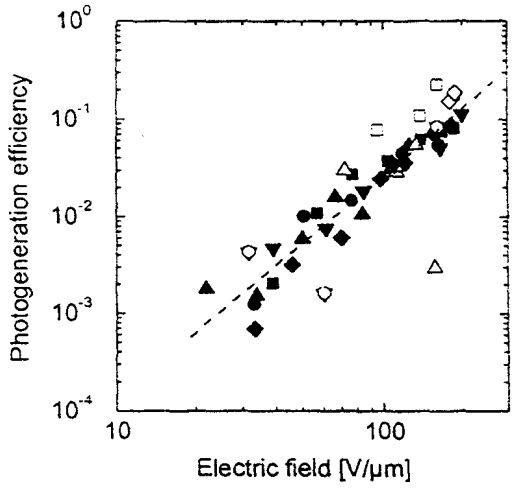

Fig 3. Field dependence of the charge carrier photogeneration efficiency h for PR blends based on PVK/TNF with different T_g and chromophore content r_{CHR}: 20 wt.-%, T_g = 59.5°C (up-triangle); 20 wt.-%, T_g = 30°C (diamonds); 20 wt.-%, T_g = 14°C (squares; 30 wt.-%, T_g = 62°C (down-triangle); 40 wt.-%, T_g = 72°C (circles). Data were obtained by xerographic discharge with illumination at 580 nm (filled symbols) and 671 nm (open symbols). h was calculated using only the absorption of the sensitizer. The dashed line indicates a power-law dependence of the efficiency on the electric field with a exponent of 2.3 [20].

The field dependence of h is well-described by Onsager's theory. Charge carrier photogeneration efficiencies in the PR blends are approximately 3 % at a field of 100 V/µm (Fig. 3), but the efficiency decreases rapidly with decreasing field to only 0.7 % at 50 V/µm. At fields between 30 and 200 V/µm, the photogeneration efficiency follows a power law

dependence h prop. E^p, with a value of the coefficient p of ca. 2.3. Further, the generation efficiency is the same for illumination with 580 nm and 671 nm.

5. SCHILDKRAUT MODEL

For a given electric field, the photogeneration efficiency h as determined by XD experiments is several orders of magnitude higher than the internal photocurrent efficiency f_{int} calculated from j_{photo} (Figs. 2 and 3). A consistent picture of the photoconductivity, the charge carrier photogeneration and the PR performance is provided by relating f_{int} to h via the trap density in the material [20].

Commonly, Kukhtarev's model for photorefractivity in inorganic crystals is used to describe the PR effect in polymeric systems [11,12]. An alternative model developed by Schildkraut *et al.* [15] includes several features typical for organic PR compounds. Its basic concept is depicted in Figure 4. Mobile holes are generated solely by photoexcitation of neutral sensitizer molecules (initial density S_i; generation rate $g(E)$). Thermal generation and charge carrier injection are neglected. Upon excitation free holes and negatively charged sensitizer molecules S^- are generated. The latter can act as recombination centers for the free holes (recombination rate r). The mobile holes might, furthermore, be captured by traps (initial density T_i; trapping rate t). Finally, trapped carriers might be detrapped by thermal activation (detrapping rate d). While the general set of coupled equations can only be solved numerically [15], Schildkraut and Cui gave zero- and first-order analytical expressions for either the case of deep traps (no detrapping) or no traps ($T = 0$).

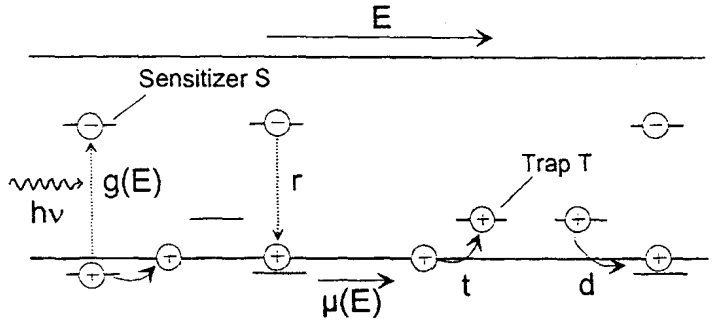

Fig. 4. Schematic representation of Schildkraut's model for the photorefractive effect in organic materials. Initially, all sensitizer molecules (initial density S_i) are neutral, and all hole traps (initial density T_i) are empty and neutral. Under illumination, holes are photogenerated with a field-dependent rate $g(E)$. For every photogenerated hole, a negatively charged sensitizer molecule is generated. The motion of the holes is described by a field-dependent mobility $m(E)$. r is the recombination rate of photogenerated holes with negatively charged sensitizer molecules. Holes can be captured by traps with a trapping rate t. The detrapping rate back to the hole transport band is d.

In a recent publication we translated the most important expressions of the model from the dimensionless form used by Schildkraut *et al.* into SI units [20]. In the limits discussed there the following expression, which related the internal photocurrent efficiency f_{int}, the charge carrier photogeneration efficiency h, and the trap density T_i in the PR material, is obtained:

$$\phi_{int} = \underbrace{\frac{\varepsilon\varepsilon_0 E_0}{eLT_i}}_{G}\eta_0 \quad . \tag{3}$$

In Eq. (3) the photoconductivity gain factor G is used to express that the number of carriers flowing through the external circuit in steady-state photoconductivity experiments, can be larger or smaller than the number of primarily photogenerated charge carriers [22,23]. Note, that an equation similar to Eq. (3) was derived by Bäuml *et al.* [10] for the

density of recombination centers, which were identified with deep traps. The derivation in this work was based on an estimate of the lifetime of a photogenerated charge carrier before being trapped in a recombination center.

In order to determine T_i we plot the internal photocurrent efficiency for different samples as a function of the electric field. This is shown in Figure 5 together with the field dependence of the charge carrier photogeneration efficiency h as derived trom XD experiments. For each data set, T_i (and thus G) was adjusted such that f_{int}/G (Eq. (3)) is in good agreement with the predictions for h from the Onsager fits of the xerographic data. Note that all data are re-scaled using only one field-independent value for T_i. The field dependence of $h(E)$ as determined by the adjusted photocurrent data is in excellent agreement with the h-E-curves predicted by Onsager's theory. This proves that Schildkraut's model is applicable for describing the photoelectric properties for 3 orders in magnitude in voltage, corresponding to ca. 3 orders of magnitude in efficiency. For all samples and voltages, G is much smaller than unity. The adjustment of the photocurrent data yields values of 1.5 - 2.0 $\times$ 10^{16} cm^{-3} for T_i. Note that this value is identical to the value determined before using a scanning-voltage experiments at fields below 3 V/μm, but lower than the density of 5 $\times$ 10^{16} cm^{-3} determined at high fields with a DC photocurrent experiment [20]. We suppose that the determination of absolute trap densities from the comparison of the photocurrent and photogeneration efficiencies is strongly affected by the exact experimental conditions, which will be subject of further investigations.

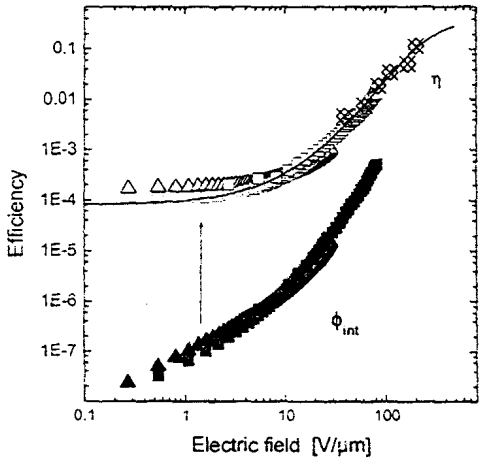

Fig. 5. A comparison of the field dependence of the photogeneration efficiency h of a samples based on PVK/TNF with 30 wt.% chromophore content determined by XD experiments (crossed diamonds) with calculated values of h (open symbols) and the internal photocurrent efficiency f_{int} (filled symbols) of samples with 30 wt.-% (squares) and 50 wt.-% (triangles) chromophore content. The values of f_{int} and h were calculated according to Eqs. (l) and (2). For each data set, the photoconductivity gain factor G was optimized using Eq. (3) to give a continuous dependence of h on the electric field. The line is a fit using Onsager's theory.

6. SPACE-CHARGE FIELD

The estimated trap density can be used to predict the first-order Fourier component of the electric space-charge field E_1 caused by illumination with a perfect sinusoidal fringe pattern [20]. Schildkraut's model was, however, developed for the external electric field E_0 parallel to the grating vector K. In DFWM and 2BC experiments on organic PR materials, the grating vector is typically tilted with respect to the external field direction by an angle j. Thus, the field component E_0 parallel to K will be smaller than the total applied external field $E_{0,T}$ according to

$$E_0 = E_{0,T} \cos j \quad . \tag{4}$$

Using Eqs. 4) and assuming (a) no field dependence of the mobility and (b) that the photogeneration rate is much smaller than the initial hole trapping rate, i.e., the limit of low density of free holes, the following relations are obtained for the amplitude $| E_{SC,1} |$ of the first Fourier component of the space-charge field and the phase shift ϕ:

$$\left|E_{SC,1}\right| = E_0 \sqrt{\frac{E_q^2}{(1+p\cos^2\varphi)^2 E_q^2 + E_0^2}} \tag{5a}$$

$$\phi = \tan^{-1}\left(\frac{E_0}{(1+p\cos^2\varphi)E_q}\right) \tag{5b}$$

with

$$E_q = \frac{e\Lambda}{2pe_0 e} T_i \quad . \tag{6}$$

Here, Λ is the grating period of the intensity grating. Note that the dependence of $| E_{SC,1} |$ on the external field E_0 in the limit of $E_0 < E_q$ is

$$|E_{SC,1}|_{E_0 < E_q} = \frac{E_0}{(1+p\cos^2 j)} \quad . \tag{7}$$

Here, the exponent p in the field dependence of the photogeneration efficiency enters in the denominator. Therefore, the model predicts a decrease of the first order Fourier component of the space-charge field, if the charge carrier photogeneration efficiency h is strongly field dependent. The reason for this is, that the space charge field becomes non-sinusoidal for $p \neq 0$. In this case, the first order Fourier component is smaller than the total space charge field, which is limited by E_0. Further, the analysis of the phase ϕ yields a modified effective saturation field in comparison to the standard model [11,24]

$$E_{q,eff} = (1 + p\cos^2\varphi)E_q \quad . \tag{8}$$

We estimated $E_{q,eff}$ based on the results of our photoelectrical experiments for parameters typically used in PR experiments: grating vector tilt angle $j = 60°$ and $L = 3$ μm. As discussed above, the trap density was set to 2×10^{16} cm^{-3} and $e = 5.5$. Furthermore, $p = 2.3$ was estimated from the field dependence of the charge carrier photogeneration efficiency (Fig. 5). Calculation with Eqs. (6) and (8) yields $E_q = 31$ V/μm and $E_{q,eff} = 49$ V/μm. The estimated value for $E_{q,eff}$ is clearly smaller than the saturation field of 120 V/μm as estimated from PR experiments. This saturation field corresponds to a larger trap density of ca. to 5×10^{16} cm^{-3}. Also note, that assumptions leading to Eq. 5 such as a constant mobility or the neglect of detrapping might not be completely full-filled in real systems.

7. RESPONSE TIME

The charge carrier photogeneration efficiency h together with the estimates for the trap density and the space-charge field in the PR materials can further be related to the speed of grating formation, which is one of the most important issues involved in device application. The formation of the light-induced grating has been investigated theoretically using Kukhtarev's model [11,25,26]. According to Yeh [16], there is a fundamental limit for grating formation given by the time required to generate the space-charge density that builds-up the steady-state space-charge field across one grating

period. All other processes, namely charge transport, charge trapping and chromophore orientation are assumed to occur instantaneously after the photogeneration of the charge carriers as any finite time involved in these processes can only lengthen the formation time of the grating. Under these assumptions the fundamental limit for the growth time is given by [16]

$$t = \frac{2\varepsilon_0 \varepsilon E_{sc}}{eL} \frac{\hbar w}{\ln 10 \alpha_{10} \eta I} \quad , \tag{9}$$

where Λ is the grating period, α the absorption coefficient, $\hbar w$ the incident photon energy, and I the intensity. Using eq. (9) the dependence of τ on the external applied field $E_{0,T}$ can be calculated. E_{SC} is computed using eq. (5a), eq. (6) is used for E_q and the data determined by xerographic discharge experiments are used for η. The other parameters are: $\varphi = 60°$, $\lambda = 632$ nm, $I = 240$ mW/cm^2, $\alpha_{10} = 10$/cm, $\varepsilon = 5.5$, $L = 3$ µm, $p = 2.3$, and $T_i = 2\times10^{16}$ cm^{-3} as used in the PR experiments The resulting field dependence of τ is shown in Fig. 6 by solid circles. It is found that the fundamental limit of speed exhibits only a rather weak field-dependence. This can be understood from the field-dependence of the two main factors in Eq. 9. On one hand, the generation efficiency η increases strongly with increasing field. The corresponding decrease in τ is, however, partially compensated by the linear increase of the space-charge field E_{SC} (for external fields smaller than the saturation field E_q).

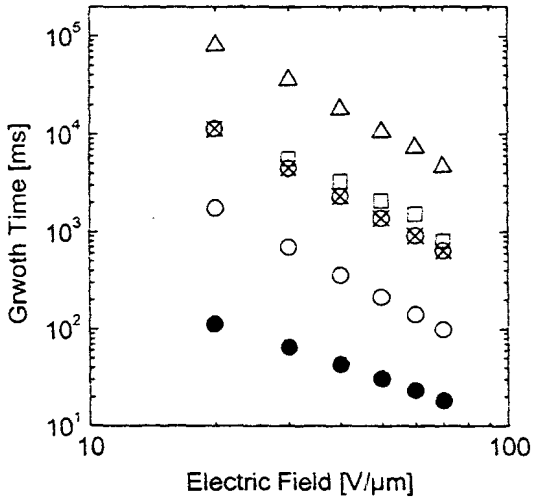

Fig. 6. Growth time t of the PR effect as determined from the analysis of transient DFWM experiments on PVK/TNF (open squares) and PVK/PCBM (open triangles) with a chromophore density of 30 wt.%. The data were fit by a multiexponential growth curve and the fastest component t_1 is plotted in the Figure as function of the applied external field. Also shown are the predictions from Eq. 9 (solid circles) according to Yeh's-mcdel and those from Eq. 10 with E_q = 31 V/µm (open circles) or E_q =200 V/µm (crossed circles), respectively.

The predicted growth rates are compared to response times derived from DFWM experiments on PVK/TNF blends. As grating formation in PR polymers involves several processes with different time constants, the fastest component t_1 is used for comparison with the fundamental limit of speed. Over the entire field range investigated here the values for t_1 are 1 - 2 orders of magnitude larger than the calculated values for t.

Alternatively, we have estimated the time, which is needed to fill the traps by the photogenerated holes.:

$$\tau = \frac{T_i}{\ln 10 \alpha_{10} \eta I / \hbar \omega} \tag{10a}$$

with Eq. 6, the following expression for the growth rate is obtained

$$t = \frac{2 p e_0 e E_q}{eL} \frac{\hbar w}{\ln 10 a_{10} h I} \tag{10b}$$

In Fig. 6 the growth times are plotted for a saturation field of 31 V/µm ($E_{q,eff}$ = 49 V/µm), corresponding to a trap density of 2.0×10^{16} cm^{-3} as determined above from PC and XD experiments. Even though the predicted values are still smaller than the experimental times, the field dependencies are identical. Perfect agreement is, however, obtained by assuming a saturation field of ca. 200 V/µm; corresponding to a trap density of ca. 13×10^{16} cm^{-3}. Even though these values are well above those measured in PR (≈ 120 V/µm) and PC experiments, the very good agreement of the measured and simulated field dependencies suggests, that trap filling rather than the build-up of the space charge field as described by Yeh's theory limits the PR response.

Figure 6 also shows the dependence of t_1 on the external applied field for the PVK/PCBM blend. The slope of the field dependence is the same as for the PVK/TNF materials. However, the response times are one order of magnitude slower than when using the TNF photosensitizer. This corresponds well to the difference in photocurrent efficiencies of the two compounds as displayed in Figure 2. The poor performance of the PVK/PCBM blend can thus be explained either by a lower photogeneration efficiency or/and by a larger trap density. Further experiments are underway to determine the generation efficiency of the PVK/PCBM PR material and to predict the growth times following the approaches outlined above.

10. CONCLUSION

Photorefractive materials based on PVK with either TNF or PCBM photosensitizers have been investigated with respect to their photoelectrical properties. It is found that the external photocurrent efficiencies can be correlated to the photogeneration efficiencies over several orders in electric field using Schildkraut's model. The comparison yields a field-independent trap density of ca. 2×10^{16} cm^{-3} for the PVK/TNF material. Further, PR growth times have been predicted by either using Yeh's model or by calculating the time needed to fill all hole traps by photogenerated holes. The results are compared to growth times *t* determined experimentally in DFWM experiments. The electric field dependence of the experimentally determined values of *t* can be well described by assuming that the fastest component of the growth of the DFWM signal is determined by the time needed to fill hole traps with a constant field-independent trap density. However, the absolute values of *t* can be explained, only, with a rather large trap density of 13×10^{16} cm^{-3}.

11. ACKNOWLEDGEMENTS

We would like to acknowledge financial support by the Volkswagen Foundation, by the Bavarian government (FORMAT program), by the European Space Agency (ESA), and by the Grant Agency of the Czech Republic (Grant No. 102/98/0696).

12. REFERENCES

1. Scott, J. C., Pautmeier, L. T. & Moerner, W. E. *J. Opt. Soc. Am. B* **19**, 2059 (1992).
2. Jones, B. E., Ducharme, S., Liphardt, M. & Goonesekera, A. *J. Opt. Soc. Am. B* **11**, 1064 - 1072 (1994).
3. Bäuml, G., Schloter, S., Hofmann, U. & Haarer, D. *Opt. Comm.* **154**, 75 - 78 (1998).
4. Sandalphon, Kippelen, B., Meerholz, K. & Peyghambarian, N. *Appl. Opt.* **35**, 2346 - 2354 (1996).

5. Grunnet-Jepsen, A., Thompson, C. L. & Moerner, W. E. *Opt. Lett.* **22**, 874 (1997).
6. Grunnet-Jepsen, A., Thompson, C. L. & Moerner, W. E. *J. Opt. Soc. Am. B* **15**, 905 (1998).
7. Schloter, S., Hofmann, U., Strohriegl, P., Schmidt, H.-W. & Haarer, D. *J. Opt. Soc. Am. B* **15**, 2473 - 2475 (1998).
8. Grunnet-Jepsen, A. et al. *Chem. Phys. Lett.* **291**, 553 - 561 (1998).
9. West, K. S. et al. *J. Appl. Phys.* **84**, 5893 - 5899 (1998).
10. Bäuml, G., Schloter, S., Hofmann, U. & Haarer, D. *Synth. Met.* **97**, 165 - 169 (1998).
11. Kukhtarev, N. V., Markov, V. B., Odulov, S. G., Soskin, M. S. & Vinetskii, V. L. *Ferroelectrics* **22**, 949 (1979).
12. Kukhtarev, N. V. in *Photorefractive materials and their applications 1* (eds. Günter, P. & Huignard, J.-P.) 99 - 129 (Springer, Berlin, 1988).
13. Chen, I., Mort, J. & Tabak, J. H. *IEEE Trans. Electron. Devices* **19**, 413 (1972).
14. Cimrová, V., Nespurek, S., Kuzel, R. & Schnabel, W. *Synth. Met.* **7**, 103 (1994).
15. Schildkraut, J. S. & Buettner, A. V. *J. Appl. Phys.* **72**, 1888 - 1893 (1992); Schildkraut, J. S. & Cui, Y. *J. Appl. Phys*. **72**, 5055 - 5060 (1992).
16. Yeh, P. *Appl. Opt.* **26**, 602 (1987).
17. Hummelen J.C., Knight B.W., LePeq F., Wudl F., *J. Org. Chem.*, 1995, **60**, 532.
18. Bittner, R., Bräuchle, C. & Meerholz, K. *Appl. Opt.* **37**, 2843 (1998).
19. Gattinger, P., Rengel, H. & Neher, D. *Synth. Met.* **83**, 245 - 247 (1996).
20. Däubler, T. K., Bittner, R., Meerholz, K., Cimrová, V. & Neher, D. *Phys. Rev. B* **61**, 13515 - 13527 (2000).
21. Andre, B., Lever, R. & Moisan, J. Y. *Chem. Phys.* **137**, 281 (1989).
22. Bube, R. H. *Photoconductivity of solids* (John Wiley & Sons, New York, 1960).
23. Däubler, T. K., Rost, H., Hörhold, H.-H. & Neher, D. *Phys. Rev. B* **59**, 1964 - 1972 (1999).
24. Grunnet-Jepsen, A., Thompson, C. L., Twieg, R. J. & Moerner, W. E. *Appl. Phys. Lett.* **70**, 1515 (1997).
25 Feinberg, J., Heiman, D., A. R. Tanguay, J. & Herrwarth, R. *J. Appl. Phys.* **51**, 1297 (1980).
26 Feinberg, J., Heiman, D., A. R. Tanguay, J. & Herrwarth, R. *J. Appl. Phys.* **52**, 537 (1981).